Anisotropic PLGA Microsphere/PVA Hydrogel Composite with Aligned Macroporous Structures for Directed Cell Adhesion and Proliferation

Shuang Liu [a, #], Xiaohu Zhou[a, #], Lei Nie [b,*], Youli Wang [c], Zhihai Hu [c], Oseweuba Valentine Okoro[d], Amin Shavandi [d,*], and Lihong Fan [a,*]

[a] School of Resources and Environmental Engineering, Wuhan University of Technology, Wuhan 430070, P. R. China

[b] College of Life Sciences, Xinyang Normal University, Xinyang 464000, China.

[c] Rizhao Biomedicine and New Materials Research, Wuhan University of Technology, Rizhao 276826, P. R. China.

[d] Université libre de Bruxelles (ULB), École polytechnique de Bruxelles - BioMatter unit, Avenue F.D. Roosevelt, 50 - CP 165/61, 1050 Brussels, Belgium.

[#] Shuang Liu and Xiaohu Zhou have the same contribution to the article.

[*] **Corresponding Authors**

Prof. Lihong Fan:

Post address: School of Resources and Environmental Engineering, Wuhan University of Technology, 122 Luoshi Road, Wuhan, Hubei, 430070, China.

E-mail address: fanlihong2000@163.com

Prof. Lei Nie:

Post address: College of Life Sciences, Xinyang Normal University (XYNU), Xinyang, 464000, China. Tel: +86-13600621068. ORCID: 0000-0002-6175-5883

E-mail address: nieleifu@yahoo.com; nielei@xynu.edu.cn

Prof. Amin Shavandi:

Post address: BioMatter unit - École polytechnique de Bruxelles, Université Libre de Bruxelles, Avenue F.D. Roosevelt, 50 - CP 165/61, 1050 Brussels, Belgium.

E-mail address: amin.shavandi@ulb.be

Abstract

The fabrication of biotissues using anisotropic constructs capable of repairing and/or replacing diseased biotissues remains a significant challenge in tissue engineering. Therefore, this study investigated the fabrication of an anisotropic PLGA-microspheres/PVA-hydrogel composite using a novel directional freezing-thawing (DFT) technique. The DFT technique altered the properties of the anisotropic PLGA-microspheres/PVA-hydrogel composite, such that its compressive strength improved from 14.64 ± 1.09 MPa after three DFT cycles to 45.77 ± 6.73 MPa after nine cycles. The utilization of the DFT technique was also shown to enhance the proliferation and adhesion of cultured chondrocyte cells. The obtained results demonstrated that DFT constituted a facile method to fabricate anisotropic microsphere/hydrogel composites with improved and directed cell adhesion characteristics.

Keywords: PVA hydrogel; anisotropic structure; PLGA microspheres; cell adhesion; cartilage

1. Introduction

The progressive destruction of articular cartilage may be caused by osteoarthritis (OA), limiting the capacity for self-repair and regeneration of damaged cartilage (1, 2). Several strategies such as osteochondral autografts, microfracture surgery, autologous chondrocyte implantation, and matrix-induced autologous chondrocyte implantation can be employed to repair minor cartilage defects (3). Recently, artificial-engineered scaffolds have been used to simulate the performance and structures of bio-tissues to regenerate damaged cartilage in the human body (4-6).

Due to the tissue-like features of cartilage, hydrogel displays potential for treating cartilage defects. However, articular cartilage is characterized by a unique structure and performance that confers it with anisotropic microstructures, mechanical behaviours, and functionalities (7, 8). Most synthetic hydrogels that have been used for biomaterials engineering are isotropic, and thus, it is desirable to create novel biomaterials with tunable anisotropic structures, properties, and functionalities (9, 10).

Several methods have been developed in the last decade to prepare hydrogels with anisotropic microstructures (11-15). For instance, the anisotropic poly(2-hydroxyethyl methacrylate) (PHEMA) hydrogels were developed by using the directional freezing, radiation-induced polymerization and crosslinking (DFRPC) technique (11, 12). Gong *et al.,* also reported an anisotropic hydrogel with photonic crystal structures produced via the uniaxial alignment of lamellar bilayers (13). Sun *et al.,* prepared a PEG hydrogel with aligned pores by combining unidirectional freezing and cryo-polymerization (14). Nevertheless, due to the uncontrollable mechanical properties and low biocompatibility,

most polymeric anisotropic hydrogels were limited for biomedical applications (16).

Poly (vinyl alcohol) (PVA) hydrogel is a three-dimensional (3D) biocompatible polymer network with high water holding capacity and high mechanical strength, which has been widely studied as a biotissue substitute (17-20). Nevertheless, pure PVA hydrogel has significant limitations, notably, the poor cell adhesion and support for cell proliferation. The biofunctionality of the PVA hydrogels can be improved using biomolecule-releasing "vehicles" such as PLGA microspheres which can facilitate protein or growth factor storage and delivery (21, 22) due to their excellent encapsulation efficiency, controllable release, and regulable degradation (23-25). Growth factors loaded PLGA microspheres could improve the adhesion, proliferation, and differentiation of stem cells on the matrix (26-29). The PLGA microspheres loaded with bone morphogenetic protein-2 (BMP-2) could induce the differentiation of human adipose-derived stem cells into osteoblasts and the formation of mature bone due to the prolonged release of BMP-2 from microspheres (30).

Protein or drug-loaded microspheres could be further composited with hydrogels to achieve controlled protein release and the sustained promotion of chondrogenesis of mesenchymal stem cells (31-34). For instance, Galeska *et al.*, controlled the release profile of dexamethasone by embedding PLGA microspheres into polyacid-containing PVA hydrogels (35). In another study, Liu *et al.*, composited PLGA nanoparticles with PVA hydrogels to regulate the insulin release rate (36). Bhardwaj *et al.*, have also prepared a composite release system based on PVA-hydrogel/PLA-microspheres for loading ibuprofen and demonstrated that the duration of the drug release could be

extended (37). In addition to drug-releasing vehicles, the potential of these microsphere/hydrogel composites for tissue engineering has also been explored. For instance, Cao *et al.*, fabricated a chondrocyte seeded PLGA microspheres/PVA hydrogel composite, which facilitated a positive outcome for cartilage repair (38). However, most of these reported microspheres/hydrogels composite with controlled biomolecule release display isotropic structures. However, anisotropic structure plays an important role in biological systems, such as mass transport, force generation, and surface lubrication. In addition, cell proliferation, migration, and differentiation are greatly influenced by such anisotropic structure (39). Thus, it is desirable to fabricate anisotropic microspheres/hydrogels composites for biomedical applications. For the first time, this work demonstrated the combination of controlled protein release and anisotropic structures of PVA hydrogels to achieve guided cell adhesion and growth. BSA-loaded PLGA microspheres were dispersed into PVA solution, then the anisotropic microspheres/hydrogels composite was fabricated by cyclic directional freezing-thawing (DFT) techniques (**Scheme 1)**.

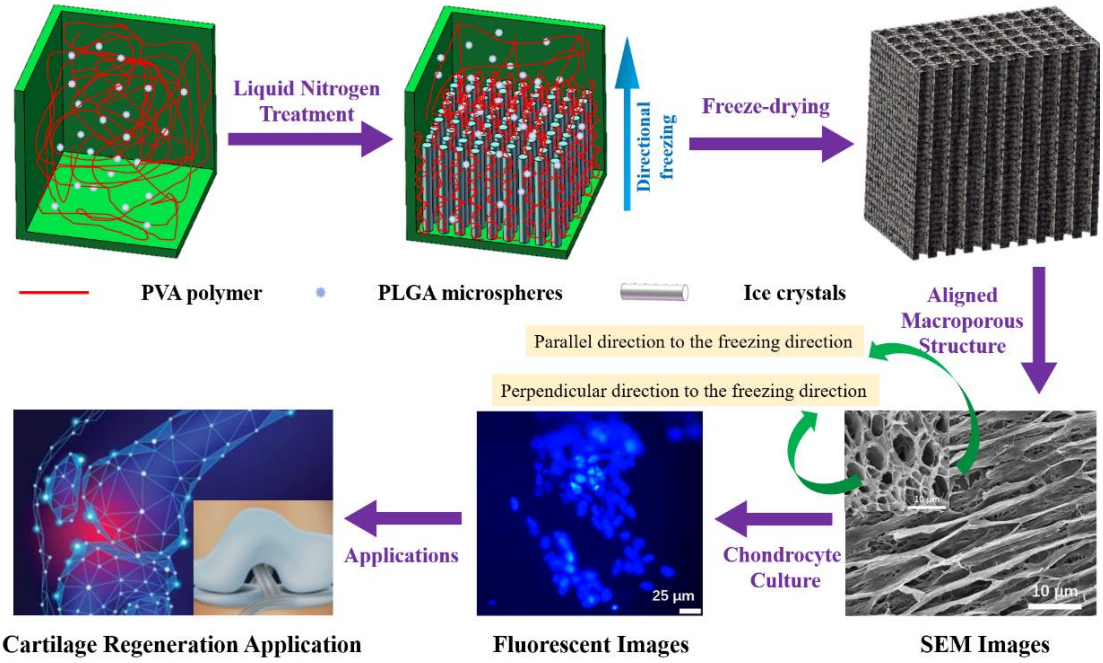

Scheme 1. Schematic illustration of the fabrication of anisotropic PLGA microspheres/PLGA hydrogel composite, the directional arranged crystalline regions in the composite was formed by DFT technique. The prepared anisotropic composite could support chondrocytes' directed adhesion and proliferation and displayed great potential for cartilage regeneration.

2. Materials and methods

2.1 Materials

Poly(D, L-lactide-co-glycolide)OH (PLGA, M_w = 50, 000; 0.35–0.45 dL/g; lactide: glycolide molar ratio 1:1) was purchased from Dai Gang Biology Co., Ltd. Polyvinyl alcohol (PVA, degree of polymerization: 1750 ± 50) was obtained from Sinopharm Chemical Reagent Co., Ltd. Bovine serum albumin (BSA, Yancheng Saibao Biotechnology Company), primary human chondrocytes (ATCC, CHON-001) and all other chemical reagents (A.R.) were used as received.

2.2 Preparation of BSA-loaded PLGA microspheres

PLGA microspheres were prepared by using a modified water-in-oil-in-water (w/o/w) double emulsion method according to our previous works (40, 41). Briefly, 150 mg PLGA was dissolved in 3 mL methylene chloride; at the same time, 90 mg of BSA was dissolved in 0.6 mL deionized water. Both solutions were mixed and emulsified using a homogenizer (QWL500C1Y, Shanghai, China) under mechanical stirring at 5000 rpm for 90 s in an ice bath. 15 mL of PVA solution (4 wt%) was poured into the resultant emulsion (w/o), followed by emulsification into a double emulsion (w/o/w) using mechanical stirring at different stirring rates (3000 rpm, 2000 rpm and 1000 rpm) for 180s at room temperature (RT, ~20 ^{o}C). Then, the double emulsion was poured into a 0.4 wt% PVA solution (300 mL), which was mechanically stirred at 800 rpm for 4 h to evaporate the organic solvent at 37 °C. The final solution was centrifuged and washed with deionized water five times and lyophilized before use. Three types of PLGA microspheres were prepared in this work with different particle sizes. The amount of BSA encapsulated in the PLGA microspheres (M_{encaps}) was calculated by subtracting the BSA amount in the solution after emulsification ($M_{residual}$) from the total feed amount (M_{feed}). The BSA encapsulation efficiency (E_{encaps}) is given as:

$$E_{encaps}(\%) = \frac{M_{feed} - M_{residual}}{M_{feed}} \times 100\%$$

The E_{encaps} value of BAS was investigated by using a BCA protein assay (42, 43).

2.3 Preparation of anisotropic PVA hydrogel

The cyclic directional freezing-thawing (DFT) technique was used to fabricate anisotropic PVA hydrogels (44). A certain amount (7.5 wt%, 10 wt%, 12.5 wt% and 15

wt%) of PVA was dissolved in deionized water at 90 °C under stirring for about 6 h. The PVA solution was injected into a mould with a 4 mm silicone spacer between two glass slides. The mould was slowly dipped into liquid nitrogen at 10 mm/min until fully immersed. Then the sample was stored in an −80 °C refrigerator for 2 h. Finally, the sample was thawed at RT for 6 h. The directional freezing-thawing process was repeated to prepare samples. The anisotropic hydrogels are denoted as DFT-C_x-N_y, where x represents the PVA concentration (wt%), and y is the number of DFT cycles. In addition, the direction parallel (//) and perpendicular (⊥) to the freezing direction were indicated.

2.4 Preparation of anisotropic microsphere/hydrogel composites

The PVA solution (10 wt%) was prepared at 90 °C and cooled to RT to fabricate hydrogels. PLGA microspheres were added to PVA solutions under magnetic stirring at 37 °C to obtain a homogeneous dispersion (microsphere/PVA × 100% = 4 wt%). The mixture was injected into a mould and immersed into liquid nitrogen for directional freezing, while the obtained hydrogels were thawed for 8 h at 37 °C. Three directional freeze-thawing cycles were applied to produce anisotropic microsphere/hydrogel composites.

2.5 Scanning electron microscopy (SEM) analysis

For SEM analysis, the PVA hydrogel and microsphere/hydrogel composites were plunged into liquid nitrogen for 15 min; then, the samples were fractured immediately. The fractured samples were freeze-dried for 36 h. The fracture surface was sputtered with a thin gold layer for imaging using a Hitachi TM-1000 scanning electron

microscope (SEM, Tokyo, Japan) at an accelerating voltage of 15.0 kV.

2.6 Compression tests

The cylindrical samples (approximately 8 mm in diameter and 8 mm in height) were tested in the unconfined compressive mode at 2.0 mm/min using an Instron 5567 mechanical testing machine equipped with a 10 kN load cell (Instron Inc, USA). Five samples were tested for each sample. The compression limit was set to 98% strain to protect the load cell.

2.7 *In vitro* release profile of BSA from PLGA microspheres

The release profile of BSA was conducted by incubating a suspension of the PLGA microspheres (20 mg of microspheres in 1 mL of PBS) in a water bath at 37 °C for 30 days. At predetermined time points, the suspensions were centrifuged, and the PBS was collected and replaced with fresh PBS. The ELISA kit was used to determine the released BSA amount in the PBS, and the microplate reader was used with the absorbance at 450 nm. Five specimens were tested for each type of microsphere.

2.8 Cell culture

Primary human chondrocytes (ATCC, CHON-001) were used to evaluate the cytocompatibility of microsphere/hydrogel composite. According to ATCC instructions, chondrocytes were cultured in McCoy's 5A medium with 10% fetal bovine serum, 100 μg mL^{-1} streptomycin, and 100 U mL^{-1} penicillin (Gibco, USA). The cells were grown under a humidified atmosphere of 95% air and 5% CO_2 at 37 °C. The medium was replaced every 2 days until 90% confluency was achieved; the cells were then passaged using 0.25% trypsin-EDTA. Cells at passage 4 were used for subsequent

experiments, described below.

2.9 Cell counting kit-8 (CCK-8) assay

The hydrogel composites were cut into slices (8 mm in diameter and 1-2 mm in thickness) and sterilized using 75 wt% ethanol for 24 h, followed by washing in sterile PBS (pH 7.4) several times replace the ethanol inside the composite. The chondrocytes (1×10^5 cells mL^{-1}) were seeded on the composite hydrogel slices in a 24-well plate (1 mL per well) and incubated in a humid atmosphere of 95% air 5% CO_2 at 37 °C. During the chondrocyte culturing, the cell medium was changed every 2 days. The viable cells grown on composites were investigated using cell counting kit-8 (CCK-8, Dojindo Molecular Technologies, Inc). After culturing for 1, 3, or 6 days, the samples were treated with CCK-8 solution for 2 h, the absorbance at 450 nm was measured using a microplate reader (SpectraMax 190, Molecular Devices, USA). PVA hydrogels without microspheres were also used for the cell culture as a comparison.

2.10 Morphology of chondrocytes on hydrogels

The directed adhesion and proliferation of chondrocytes on the composite hydrogels were investigated by fluorescent microscopy and SEM. After the cells-seeded composites were cultured for 1, 3, and 6 days, the cell-seeded samples were retrieved from the culture plate and gently rinsed using PBS and were fixed by 2.5% glutaraldehyde overnight. After the samples were rewashed with PBS, 40 μL of 4’,6-diamidino-2-phenylindole (DAPI, 10 μg/mL, Thermo Scientific™) was added in the dark and incubated for 5 min. The fluorescent images of DAPI-stained samples were obtained using Confocal Laser Scanning Microscope (CLSM, Leica TCS SP5 II,

Germany). After the fluorescent investigation, the cell-seeded samples were subsequently dehydrated in ethanol solutions using different concentrations (*i.e.* 30%, 50%, 70%, 90%, and 100%, respectively). Finally, the treated samples were sputter-coated with a thin gold layer for SEM investigation.

2.11 Statistics

All experiments were conducted in triplicate, with the data reported as means with standard deviation. SPSS software (SPSS Inc, Chicago IL) was used for the analysis. Analysis of variance (ANOVA) statistical analyses and Tukey's test were applied to investigate specific differences. Statistical significance was defined at a p-value of < 0.05 for 95% confidence.

3. Results and discussion

The pure PVA hydrogels and microspheres/hydrogel composite were fabricated using the directional freezing-thawing (DFT) method, resulting in constructs with an aligned structure to guide cell adhesion and proliferation (**Scheme 1**). There is a significant difference between the thermal conductivity of ice (2.18 W/m K) and PVA (0.2 W/m K), resulting in a temperature gradient between the ice crystals and the vicinal PVA-rich regions when the aqueous PVA solution is being frozen directionally (45). As a result, the crystallization of water into ice will occur faster than the crystallization of PVA, and consequently, the PVA chains are expelled from ice (18). Meanwhile, a temperature gradient perpendicular to the freezing direction can also form between the ice and the vicinal PVA-rich regions, leading to the crystallization of PVA chains along

the temperature gradient (46). The prepared hydrogels had an apparent channel arrangement structure parallel to the freezing direction with uniform size, and the arranged pore structure was perpendicular to the freezing direction, as shown in **Fig. 1**.

3.1. Anisotropic PVA hydrogels

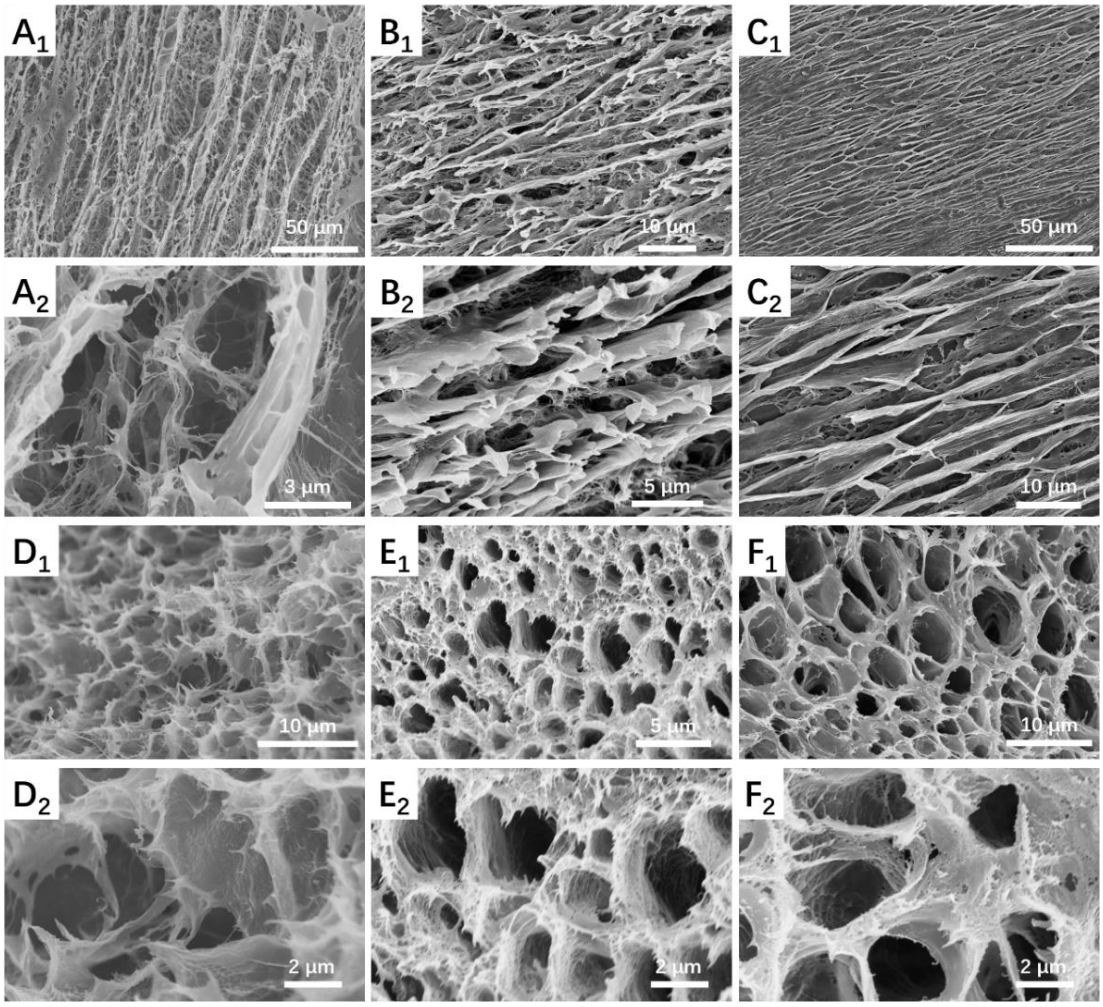

Fig. 1 SEM images of anisotropic PVA hydrogels along with the directions parallel (images A_1, B_1, C_1, A_2, B_2, and C_2) and perpendicular (images D_1, E_1, F_1, D_2, E_2, and F_2) to the freezing direction. DFT-C_{10}-N_1: (10 wt% of PVA, and DFT cycle is 1, shown in images A_1, D_1, A_2, D_2); DFT-C_{10}-N_3: (10 wt% of PVA, and DFT cycle is 3, shown in images B_1, E_1, B_2, and E_2); DFT-C_{10}-N_5: (10 wt% of PVA and DFT cycle is 5, shown in images C_1, F_1, C_2, and F_2). A_2, B_2, C_2, D_2, E_2, and F_2 images were enlarged from A_1, B_1, C_1, D_1, E_1, and F_1 images at higher

magnifications.

Fig. 1 shows the microstructures of anisotropic PVA hydrogels parallel and perpendicular to the DFT direction. The SEM images confirmed that typical anisotropic porous-channel microstructures characterized the PVA hydrogels. The microstructure of long aligned channels was similar to the "fish-bone" and was found in parallel with the dipping direction (temperature gradient direction) (**Fig. 1A$_1$–C$_2$**). The fibre-like pore morphology was observed to form as the freeze-thawing cycle number increased gradually. However, no alignment structure was found perpendicular to the temperature gradient (**Fig. 1D$_1$–F$_2$**). The result also showed that as the number of freeze-thawing cycles increased, the average pore diameters also increased from 1–2 μm for the DFT-C_{10}-N_1 hydrogel (Fig. 1d) to 2–4 μm for the DFT-C_{10}-N_3 hydrogel (Fig. 1e), and 4–8 μm for the DFT-C_{10}-N_5 hydrogel (Fig. 1f).

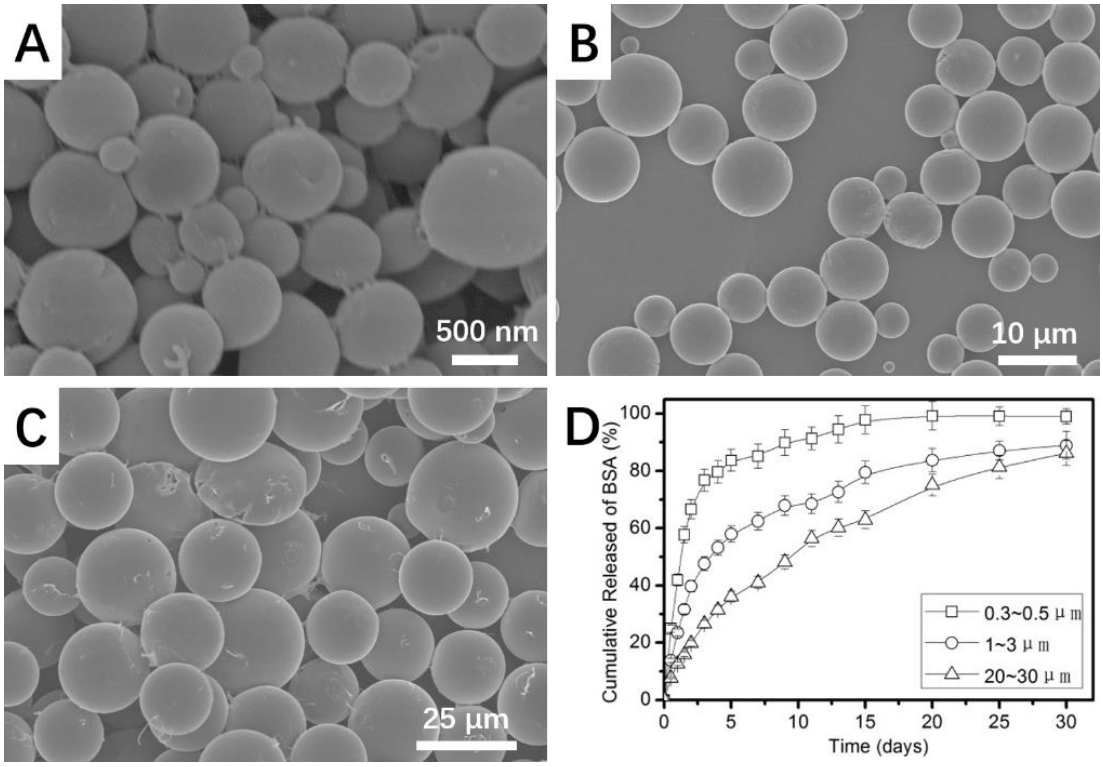

Fig. 2 (A-C) SEM images of PLGA microspheres with different sizes. (D) The release profiles

of BSA from the PLGA microspheres with different particle sizes. The error bars represent the standard deviations with $n = 5$ for each sample.

3.2. PLGA microspheres and release profile of BSA

The PLGA microspheres were prepared using a double emulsion method, and BSA was encapsulated during the formation of microspheres. Three types of microspheres with different diameters were subsequently obtained, as shown in **Fig. 2A-C**. The SEM images showed that the mechanical stirring rate could regulate the diameter of PLGA microspheres during the emulsion process. The average diameter of PLGA microspheres was increased from 0.3~0.5 μm to 20~30 μm as the stirring rate decreased from 3000 rpm to 1000 rpm. The diameter of PLGA microspheres influences the encapsulation efficiency and release behaviour of BSA. The encapsulation efficiencies of BSA for PLGA microspheres with diameters of 0.3~0.5 μm, 1~3 μm, and 20~30 μm were around 52 ± 2.1 %, 49 ± 2.8 %, and 43 ± 1.7 %, respectively. This observation indicated an inverse correlation between the diameter of PLGA microspheres and the BSA encapsulation efficiency (**Fig. 2D)**. The burst release of BSA occurred within 1–2 days. Compared to other PLGA microspheres (47), the microsphere with a smaller diameter ranging from 03-0.5 μm showed a higher release rate of 20-30 μm and reached an earlier maximum-release volume 03-0.5 μm in 15 days. The burst release of BSA is due to the large osmotic pressure between the microsphere inside and the external environment(48). Our previous work demonstrated the dependence of protein release on the particle size, where the smaller microspheres had

a higher protein encapsulation (49). As a result, the osmotic pressure between the buffer solution and microspheres is high with 0.3-0.5 μm, which reaches over 90% release efficiency at day 5.

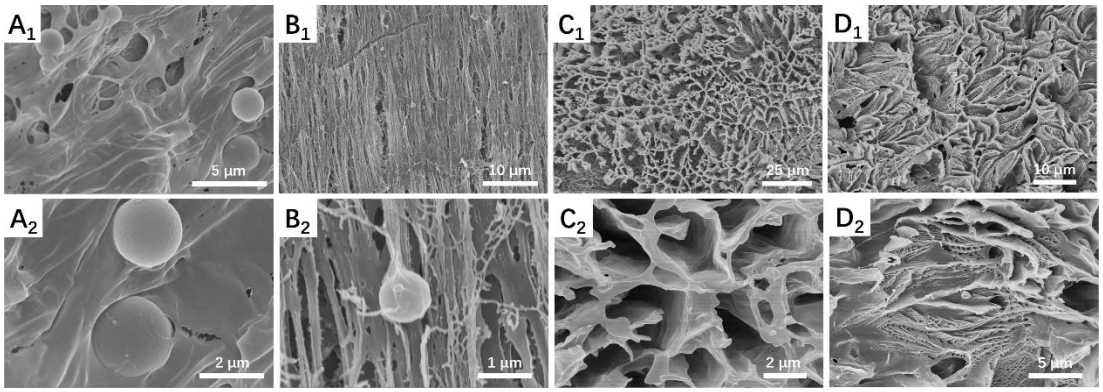

Fig. 3 SEM images of (A_1 and A_2) isotropic and (B_1, C_1, D_1, B_2, C_2, and D_2) anisotropic PLGA microsphere/hydrogel composites. Pictures B_1 and B_2 are SEM images of microsphere/hydrogel composites along with the directions parallel to the freezing direction, pictures C_1 and C_2 are SEM images perpendicular to the freezing direction, and pictures D_1 and D_2 are SEM images that along with the freezing direction at 45°. A_2, B_2, C_2, and D_2 images were enlarged from A_1, B_1, C_1, and D_1 images at higher magnifications.

3.3. Microstructure of anisotropic PLGA microspheres/hydrogel composite

The microstructure of the anisotropic composite was investigated using SEM images (**Fig. 3)**. PLGA microspheres with a diameter of 1~3 μm were used to fabricate anisotropic microspheres/hydrogel composite. The diameter of the microsphere dispersed in the PVA matrix did not influence the mechanical properties and cytocompatibility of the composite (48). The isotropic microspheres/hydrogel composite showed a non-uniform distribution of the PLGA microspheres in the PVA

matrix, and the microstructure with long aligned channels was not observed (**Fig. 3A$_1$ and 3A$_2$**). In contrast, the DFT-treated microspheres/hydrogel composite showed an anisotropic structure with highly aligned channels, and the PLGA microspheres were dispersed in the polymer matrix. Only a few microspheres were shown in **Fig. 3B$_1$-D$_2$**, mainly because the microspheres were encapsulated into the polymer network.

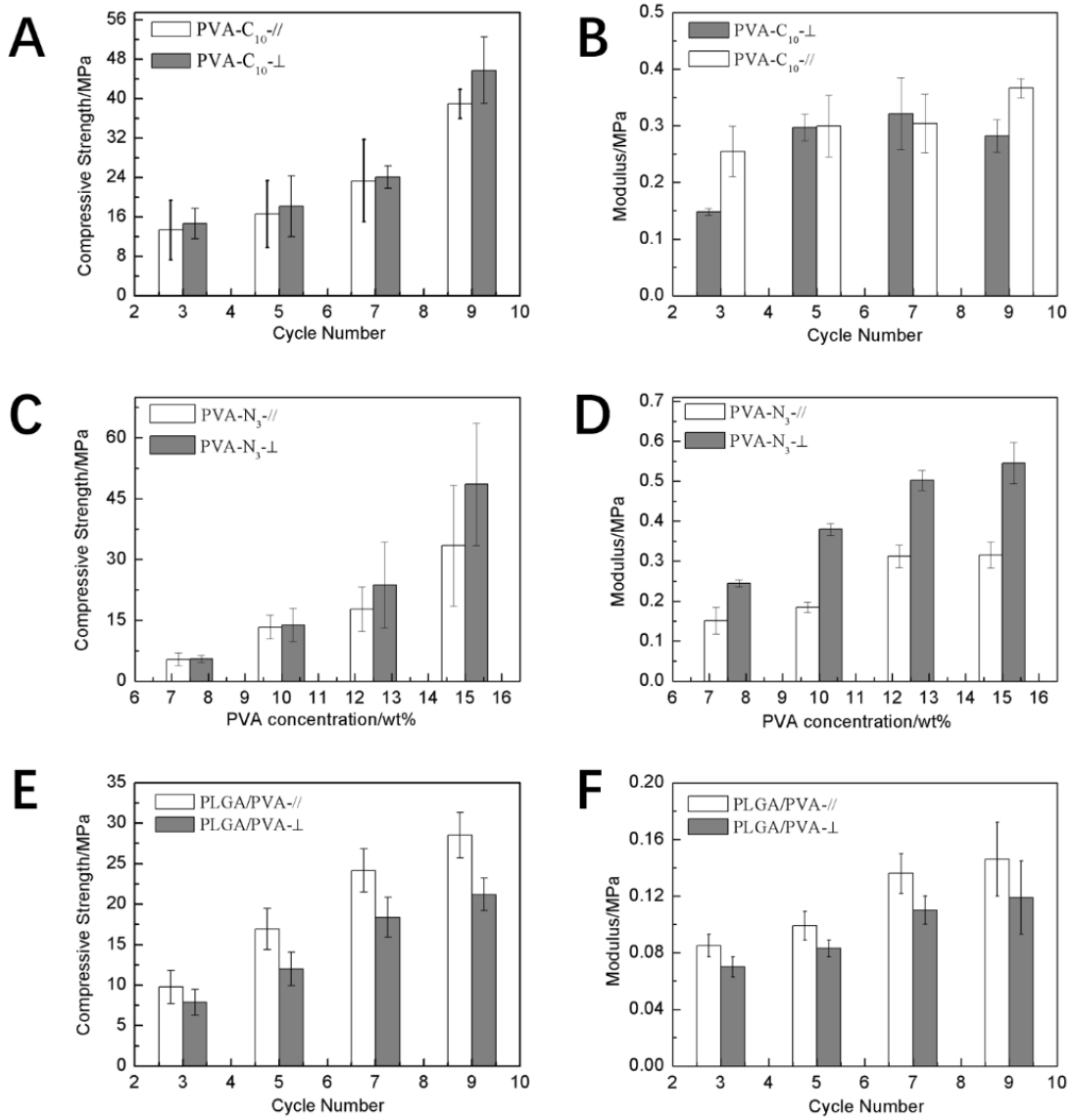

Fig. 4 The compressive strength (A) and modulus (B) of the anisotropic PVA hydrogels using 10 wt% of PVA (x=10) as a function of the DFT cycle number. The compressive strength (C) and modulus (D) of the anisotropic PVA hydrogels using DFT cycle at 3 (y=3) as a function of

PVA concentration. The compressive strength (E) and modulus (F) of the anisotropic microsphere/hydrogel composites as a function of DFT cycles number.

3.4. Mechanical anisotropy of microspheres/hydrogel composite

The direction-related compression tests were used to characterize the mechanical anisotropy of the DFT-treated PVA hydrogels and microsphere/hydrogel composite (**Fig. 4**). The samples were cut parallel with or perpendicular to the freezing direction. The compressive strength (σ) and modulus (E) of the PVA (DFT-C_{10}) hydrogels are shown in **Fig. 4A** and **Fig. 4B**. The compression properties of the PVA hydrogels varied with the number of DFT cycles. In the parallel direction (**Fig. 4A**), the compressive strength (σ//) was observed to increase significantly from 13.36 ± 2.97 MPa for 3 DFT cycles to 38.95 ± 6.07 MPa at 9 cycles. In the perpendicular direction (**Fig. 4B**), compressive strength was significantly increased from 14.64 ± 1.09 MPa at 3 DFT cycles to 45.77 ± 6.73 MPa at 9 cycles. In addition, the compressive strength of PVA hydrogels in parallel and perpendicular to the DFT directions were significantly different. For the PVA hydrogels prepared with a certain DFT cycle number, the σ in the perpendicular direction ($\sigma_{\perp}$) was usually higher than those in the parallel direction ($\sigma_{//}$). In contrast, the modulus (E) in the perpendicular direction ($E_{\perp}$) was observed to be lower than that in the parallel direction ($E_{//}$).

The compressive strength (σ) and modulus (E) of DFT-treated PVA hydrogels varied depending on the concentration of PVA (7.5 wt%, 10 wt%, 12.5 wt%, 15 wt%), (**Fig. 4C** and **Fig. 4D**). For the PVA hydrogels treated with the same DFT cycles (*e.g.*,

n=5), in the perpendicular direction, the compressive strength was significantly increased from 6.87± 0.66 MPa for 7.5 wt% of PVA concentration to 46.71 ± 7.01 MPa for 15 wt% PVA concentration. The modulus was significantly increased from 0.21± 0.06 MPa to 0.53 ± 0.09 MPa. Moreover, these values were higher in the perpendicular direction than those in the parallel direction. The compressive strength was 46.71 ± 7.01 MPa in the perpendicular direction, and the compressive strength in the parallel direction was 32.28 ± 11.69 MPa for the sample using 7.5 wt% of PVA concentration.

Next, the compressive strength and modulus of microspheres/hydrogels composite were evaluated, as shown in **Fig. 4E** and **Fig. 4F**. The mechanical properties of microspheres/hydrogels composite could be enhanced by increasing DFT cycle number. By adding PLGA microspheres to the PVA hydrogels with 9 DFT cycle number, the compressive strength decreased from 45.77 ± 6.73 MPa to 19.67 ± 1.59. No chemical interaction or affinity between the PLGA microspheres and the PVA matrix was observed (50). It was likely that the PLGA microspheres embedded in the hydrogels might introduce structural defects, and as a result, the compressive strength of microspheres/hydrogels composite was decreased.

On the other hand, with the presence of PLGA microspheres, the compressive strength of microspheres/hydrogels composite in parallel direction became higher than that in the perpendicular direction (**Fig. 4D**), in contrast to those for pure DFT-treated PVA (**Fig. 4A** and **4C**). The presence of microspheres improved the hydrogel in the vertical direction, while in the parallel direction, changes in the mechanical properties were inconsistent, with the reduction of compressive strength. The decrease of the

mechanical properties maybe because most of the microspheres were embedded into the polymer matrix instead of the pores. The compression perpendicular to the alignment may easily cause fracture since the microspheres act as structural defects. In contrast, compressive loading along with the alignment may encounter much fewer structural defects (51).

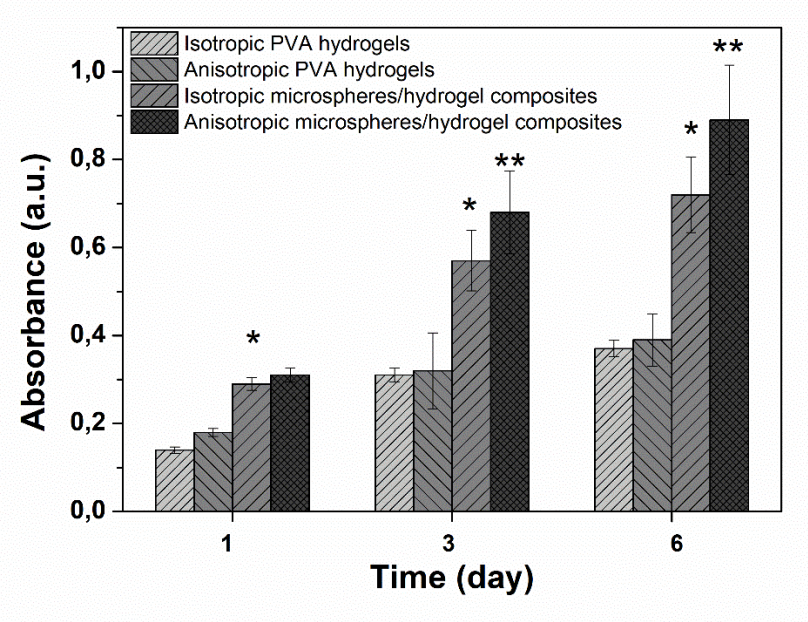

Fig. 5 Cytocompatibility of isotropic PVA hydrogels, anisotropic PVA hydrogels, isotropic and anisotropic PLGA-microsphere/PVA-hydrogel composites (DFT-C_{10}-N_5, 10 wt% of PVA, and DFT cycle is 5), which were evaluated using CCK-8 assay through culturing with chondrocytes for 1, 3, and 6 days. *$p < 0.05$, and **$p < 0.05$.

3.5. Guided cell adhesion and proliferation on the anisotropic microspheres/hydrogel composite

As an intrinsically non-cell adhesive scaffold, it is difficult for PVA hydrogel to support cell proliferation and differentiation, limiting its applications as biotissue

substitutes. It was proved that the chondrocytes adhesion and proliferation on PVA hydrogels could be enhanced by compositing with protein-loaded microspheres (52). This work quantitatively assessed the cytocompatibility of isotropic and anisotropic microsphere/hydrogel composites using the CCK-8 assay (**Fig. 5**). The absorbance at 450 nm was used to determine the cell density in the samples. There was a slight cell number increase over days for both isotropic and anisotropic PVA hydrogels. However, the chondrocyte density growths on isotropic and anisotropic PLGA-microsphere/PVA-hydrogel composites were higher over days than cells grown on pure PVA hydrogel. The anisotropic PLGA-microsphere/PVA-hydrogel composites (DFT-C_{10}-N_5) showed the highest cell density.

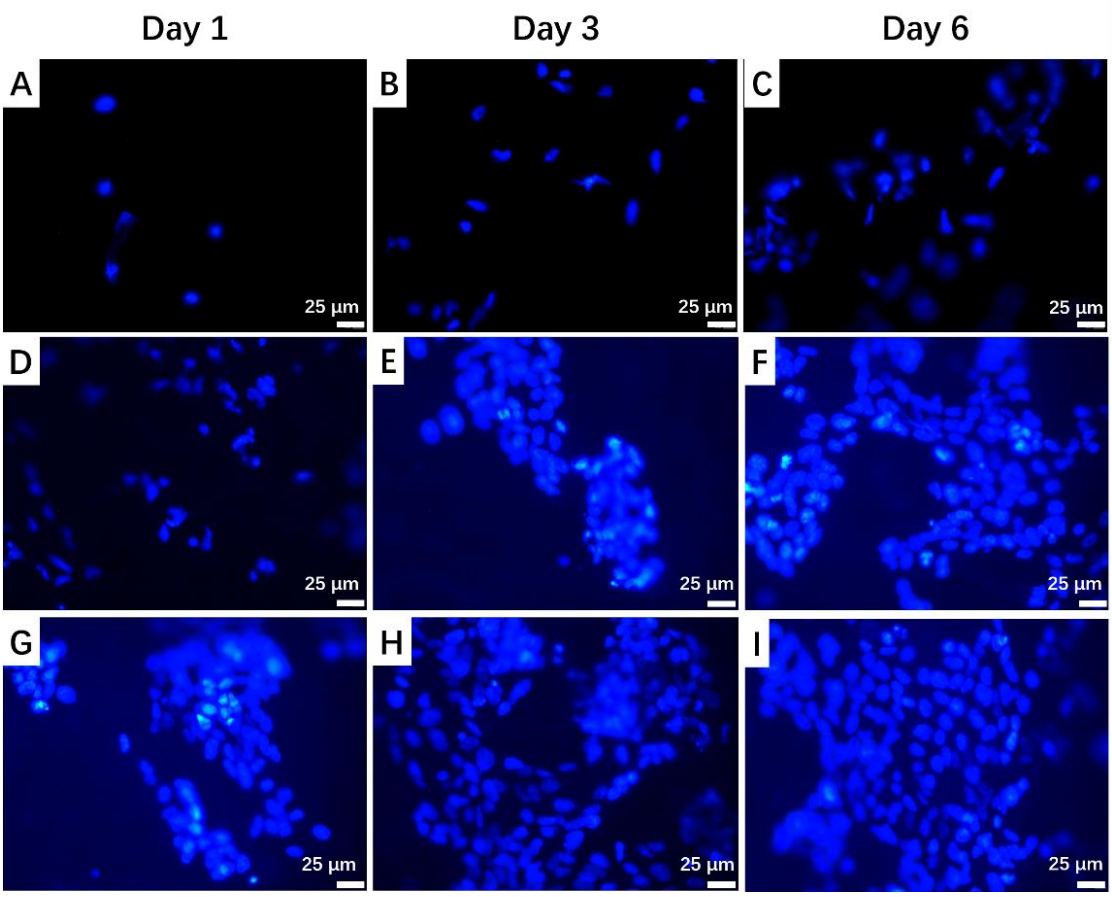

Fig. 6 Representative fluorescent microscopy images of chondrocytes cultured on (A-C)

anisotropic PVA hydrogel (DFT-C_{10}-N_5, 10 wt% of PVA, and DFT cycle is 5), isotropic (D-F) and (G-I) anisotropic PLGA-microsphere/PVA-hydrogel composites (DFT-C_{10}-N_5) for 1, 3, and 6 days. The chondrocytes nucleus were stained by DAPI and displayed in blue colour.

Furthermore, the morphology of chondrocyte adhered and proliferated on microspheres/hydrogel composites was assessed using fluorescent microscopy images. **Fig. 6** displayed the confocal microscopy images of DAPI-stained chondrocytes cultured on PVA hydrogels and composites for 1, 3, and 6 days. For anisotropic PVA hydrogel, a few chondrocytes were observed after 6 days of culture, mainly due to the intrinsical non-cell-adhesive characteristic of the pure PVA (**Fig. 6A-C**). In contrast, the use of PLGA-microspheres/PVA-hydrogel composite (4 wt% PLGA microspheres) as scaffolds favours cell attachment and growth, as illustrated by increased cell number density as the culture time increased from day 1 to day 6. The cell number on PLGA-microspheres/PVA-hydrogel composite increased faster than pure PVA hydrogel (**Fig. 6D-I**). The highest chondrocyte number was observed on anisotropic PLGA-microsphere/PVA-hydrogel composites and is consistent with the CCK-8 assay result (**Fig. 5**). The cell adhesion and proliferation on the PLGA-microsphere/PVA-hydrogel composites are explained as 1) the PLGA microspheres added to the hydrogels improve the roughness of the hydrogel surface, which is conducive to cell adhesion; 2) The release of BSA from the PLGA microspheres favours cell proliferation and adhesion (49). Interestingly, the chondrocytes showed a guided distribution on anisotropic PLGA-microsphere/PVA-hydrogel composites due to the anisotropic microporous structures.

In addition, the chondrocyte morphology and distribution on scaffolds were revealed using SEM images shown in **Fig. 7**. After culturing with chondrocyte for 6 days, few cells were observed on pure PVA hydrogel (**Fig. 7A**). On the contrary, many chondrocytes were observed on isotropic and anisotropic PLGA-microsphere/PVA-hydrogel composites (DFT-C_{10}-N_5) (**Fig. 7B** and **7C**). These results are consistent with the fluorescent microscopy images. Interestingly, the main structure of the PLGA microsphere in composites was well-maintained after culturing with chondrocytes which could cause the release of BSA to slow down. However, some pores on the surface of PLGA microspheres were formed due to BSA's degradation and release (**Fig. 7D**).

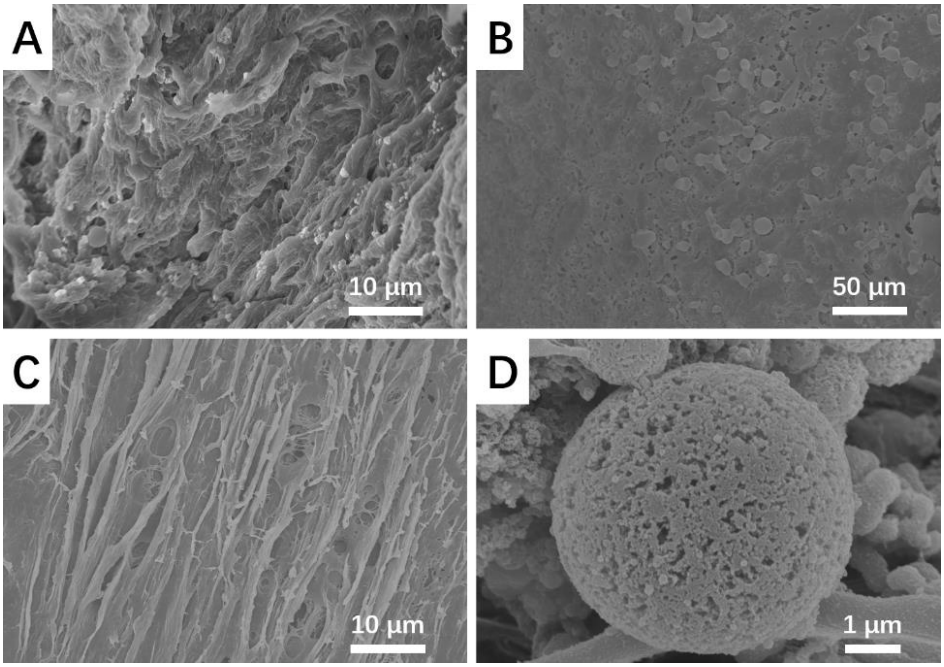

Fig. 7 SEM images of chondrocytes cultured on PVA hydrogel (A), isotropic (B) and (C) anisotropic PLGA-microsphere/PVA-hydrogel composites (DFT-C_{10}-N_5, 10 wt% of PVA, and DFT cycle is 5) for 6 days. The morphology of PLGA microspheres in composites after culturing with chondrocytes at day 6.

The fabrication of anisotropic hydrogels has been recently reported in terms of microstructures, mechanical properties, and/or optical properties(46). The directional freeze-thawing (DFT) method has been demonstrated to create anisotropic hydrogels with highly aligned structures(53). PVA hydrogels have been widely used for potential applications as biosubstitutes for their outstanding biocompatibility, strength, toughness, and lubricity (54-56). Many efforts have been endowed to improve its bio-functionality by compositing with biomolecules (35, 57, 58). Herein, for the first time, we have successfully demonstrated a combination of controlled protein release and anisotropic structures of tough PVA hydrogels. By using the DFT method, anisotropic structures were formed. It was shown that the anisotropy in terms of pore orientation and mechanical strength could be adjusted by controlling the freezing direction, PVA concentration, and DFT cycle number.

Moreover, the average pore size could be regulated by DFT cycle number. It is known that the porous size and modulus of the substrate have essential influences on cell adhesion and growth (59, 60). The average pore size of 4-8 μm was favourable for the chondrocyte adhesion. The results demonstrated the enhanced chondrocyte adhesion and growth on the PLGA-microspheres/PVA-hydrogel composite. Moreover, the growth of chondrocytes showed a strong correlation to the highly aligned microporous structures.

4. Conclusions

This study demonstrated that a microsphere/hydrogel composite with highly

aligned structures could support cell-directed adhesion and growth. The morphology and alignment extent of composite could be regulated by controlling the dipping rate of hybrid solution into liquid nitrogen. In addition to the aligned microstructures, the anisotropic mechanical properties of the prepared composite were demonstrated by performing compressive tests parallel with and perpendicular to the freezing direction. The results displayed that the compressive strength and modulus of anisotropic pure PVA hydrogels and microspheres/hydrogel composite were both increased by increasing freezing-thawing cycling number and PVA concentration. Lastly, the cultured chondrocyte number on anisotropic microspheres/hydrogel composite increased more rapidly than the cultured chondrocyte number on anisotropic pure PVA hydrogels and isotropic microspheres/hydrogel composite. Significantly, the chondrocyte could be directedly adhered and proliferated on anisotropic microspheres/hydrogel composite, mainly because BSA was gradually released from PLGA microspheres over days. The obtained results demonstrated a facile method to fabricate anisotropic microsphere/hydrogel composite with improved and directed cell adhesion.

Acknowledgements

We are grateful for financial support from the National Natural Science Foundation of China (51773161), and the Technological Innovation Project of Rizhao City (2019CXZX1108).

Conflict of Interest

The authors declare that they have no conflict of interest.

References

1. Martín, A. R., Patel, J. M., Zlotnick, H. M., Carey, J. L. and Mauck, R. L., npj Regenerative Medicine. 4, 12 (2019).
2. Xavier, H., Mary, B. G. and Francis, B., Current Rheumatology Reports. (2013).
3. Wei, W., Ma, Y., Yao, X., Zhou, W., Wang, X., Li, C., Lin, J., He, Q., Leptihn, S. and Ouyang, H., Bioact Mater. 6, 998-1011 (2021).
4. Do Kyung, K., Jeong In, K., Bo Ra, S. and Gilson, K., Materials Science and Engineering: C. (2017).
5. Xuan, Z., Sara, T., Timothy, E., Sung Yun, H., Haitao, C., Thomas, J. W., Hicham, F. and Lijie Grace, Z., ACS Applied Materials & Interfaces. (2020).
6. Silvia, B., Martina, C., Elena, S., Silvia, T., Veronica, M., Raffaele De, C. and Andrea, P., Processes. (2021).
7. Wang, X. Z., Wang, H. L. and Brown, H. R., Soft Matter. 7, 211-219 (2011).
8. Wu, D. J., Vonk, N. H., Lamers, B. A. G., Castilho, M., Malda, J., Hoefnagels, J. P. M. and Dankers, P. Y. W., Eur Polym J. 141, (2020).
9. Zhang, H. and Cooper, A. I., Advanced Materials. 19, 1529-1533 (2007).
10. Zhang, H. F., Hussain, I., Brust, M., Butler, M. F., Rannard, S. P. and Cooper, A. I., Nature Materials. 4, 787-793 (2005).
11. Chen, M., Zhu, J., Qi, G., He, C. and Wang, H., Materials Letters. 89, 104-107 (2012).
12. Zhu, J., Wang, J., Liu, Q., Liu, Y., Wang, L., He, C. and Wang, H., Journal of Materials Chemistry B. 1, 978 (2013).
13. Haque, M. A., Kurokawa, T. and Gong, J. P., Soft Matter. 8, 8008 (2012).
14. Wu, J., Lin, Y. and Sun, J., Journal of Materials Chemistry. 22, 17449 (2012).
15. Wang, T. W., Zhang, F., Zhao, R., Wang, C., Hu, K. H., Sun, Y., Politis, C., Shavandi, A. and Nie, L., Des Monomers Polym. 23, 118-133 (2020).
16. Sano, K., Ishida, Y. and Aida, T., Angew Chem Int Edit. 57, 2532-2543 (2018).
17. Gong, J. P. and Osada, Y., Adv Polym Sci. 236, 203-246 (2010).
18. Xu, Y. C., Yin, H. Y., Chu, J., Eglin, D., Serra, T. and Docheva, D., Biomater Sci-Uk. 9, 1237-1245 (2021).
19. Nie, L., Deng, Y. L., Li, P., Hou, R. X., Shavandi, A. and Yang, S. F., Acs Omega. 5, 10948-10957 (2020).
20. Nie, L., Li, X. C., Wang, Z., Hu, K. H., Cai, R. H., Li, P., Han, Y. T., Sun, M., Yuan, H. Y., Suo, J. P. and Yang, S. F., Bioinspir Biomim Nan. 9, 122-128 (2020).
21. Sinha, V. R. and Trehan, A., Journal of Controlled Release. 90, 261-280 (2003).
22. Barbosa-Alfaro, D., Andres-Guerrero, V., Fernandez-Bueno, I., Garcia-Gutierrez, M. T., Gil-Alegre, E., Molina-Martinez, I. T., Pastor-Jimeno, J. C., Herrero-Vanrell, R. and Bravo-Osuna, I., Pharmaceutics. 13, (2021).
23. Nishida, A., Yamada, M., Kanazawa, T., Takashima, Y., Ouchi, K. and Okada, H., International

journal of pharmaceutics. 407, 44-52 (2011).
24. Mohammadpour, F., Kamali, H., Hadizadeh, F., Bagheri, M., Shiadeh, S. N. R., Nazari, A., Oroojalian, F. and Khodaverdi, E., J Pharm Innov. (2021).
25. Wu, Y. M., Du, D. M., Chen, J. P. and Liu, C. L., Biomed Pap. 165, 57-63 (2021).
26. Ashton, R. S., Banerjee, A., Punyani, S., Schaffer, D. V. and Kane, R. S., Biomaterials. 28, 5518-5525 (2007).
27. Spiller, K. L., Liu, Y., Holloway, J. L., Maher, S. A., Cao, Y. L., Liu, W., Zhou, G. D. and Lowman, A. M., Journal of Controlled Release. 157, 39-45 (2012).
28. Cun, D. M., Jensen, D. K., Maltesen, M. J., Bunker, M., Whiteside, P., Scurr, D., Foged, C. and Nielsen, H. M., Eur J Pharm Biopharm. 77, 26-35 (2011).
29. Chen, D., Zhang, C. X., Huo, H. J., Ji, C. C., Sun, M. and Nie, L., Materials Letters. 229, 138-141 (2018).
30. Jeon, B. J., Jeong, S. Y., Koo, A. N., Kim, B. C., Hwang, Y. S. and Lee, S. C., Macromol Res. 20, 715-724 (2012).
31. Kim, S. E., Park, J. H., Cho, Y. W., Chung, H., Jeong, S. Y., Lee, E. B. and Kwon, I. C., Journal of Controlled Release. 91, 365-374 (2003).
32. Zhao, Y. Z., Chen, R., Xue, P. P., Luo, L. Z., Zhong, B., Tong, M. Q., Chen, B., Yao, Q., Yuan, J. D. and Xu, H. L., Mat Sci Eng C-Mater. 122, (2021).
33. Feng, S. B., Nie, L., Zou, P. and Suo, J. P., J Microencapsul. 32, 201-209 (2015).
34. Oliveira, E. R., Nie, L., Podstawczyk, D., Allahbakhsh, A., Ratnayake, J., Brasil, D. L. and Shavandi, A., International Journal of Molecular Sciences. 22, (2021).
35. Galeska, I., Kim, T. K., Patil, S. D., Bhardwaj, U., Chatttopadhyay, D., Papadimitrakopoulos, F. and Burgess, D. J., Aaps J. 7, E231-E240 (2005).
36. Liu, J., Zhang, S. M., Chen, P. P., Cheng, L., Zhou, W., Tang, W. X., Chen, Z. W. and Ke, C. M., J Mater Sci-Mater M. 18, 2205-2210 (2007).
37. Bhardwaj, U., Sura, R., Papadimitrakopoulos, F. and Burgess, D. J., International journal of pharmaceutics. 384, 78-86 (2010).
38. Cao, Y., Xiong, D. S., Niu, Y. X., Mei, Y., Yin, Z. W. and Gui, J. C., Journal of Applied Polymer Science. 131, (2014).
39. Marelli, B., Ghezzi, C. E., James-Bhasin, M. and Nazhat, S. N., Biomaterials. 37, 183-193 (2015).
40. Lee, J., Oh, Y. J., Lee, S. K. and Lee, K. Y., Journal of Controlled Release. 146, 61-67 (2010).
41. Feng, S., Nie, L., Zou, P. and Suo, J., J Microencapsul. 32, 201-209 (2015).
42. Chandrasiri, I., Abebe, D. G., Loku Yaddehige, M., Williams, J. S. D., Zia, M. F., Dorris, A., Barker, A., Simms, B. L., Parker, A., Vinjamuri, B. P., Le, N., Gayton, J. N., Chougule, M. B., Hammer, N. I., Flynt, A., Delcamp, J. H. and Watkins, D. L., Acs Appl Bio Mater. 3, 5664-5677 (2020).
43. Nie, L., Zhang, G. H., Hou, R. X., Xu, H. P., Li, Y. P. and Fu, J., Colloid Surface B. 125, 51-57 (2015).
44. Zhang, L., Zhao, J., Zhu, J., He, C. and Wang, H., Soft Matter. 8, 10439 (2012).
45. Zhu, J., Wang, J., Liu, Q., Liu, Y., Wang, L., He, C. and Wang, H., J Mater Chem B. 1, 978-986 (2013).
46. Sun, Z. F., Yamauchi, Y., Araoka, F., Kim, Y. S., Bergueiro, J., Ishida, Y., Ebina, Y., Sasaki, T., Hikima, T. and Aida, T., Angew Chem Int Edit. 57, 15772-15776 (2018).
47. Jiang, C. J., Teng, L. S., Teng, L. R., Li, C. M. and Li, Y. X., J Biotechnol. 136, S416-S417 (2008).
48. Shen, J. and Burgess, D. J., Int J Pharmaceut. 429, 168-168 (2012).

49. Zhang, G.-H., Hou, R.-X., Zhan, D.-X., Cong, Y., Cheng, Y.-J. and Fu, J., Chinese Chemical Letters. 24, 710-714 (2013).
50. Liu, X., Fundora, K. A., Zhou, Z., Miller, A. L., 2nd and Lu, L., Tissue Eng Part A. 25, 172-182 (2019).
51. Xu, Y., Yin, H., Chu, J., Eglin, D., Serra, T. and Docheva, D., Biomater Sci. 9, 1237-1245 (2021).
52. Nie, L., Zhang, G., Hou, R., Xu, H., Li, Y. and Fu, J., Colloids Surf B Biointerfaces. 125, 51-57 (2015).
53. Wu, L. J., Huang, S. Q., Zheng, J., Qiu, Z. J., Lin, X. L. and Qin, Y. L., Int J Biol Macromol. 140, 538-545 (2019).
54. Jiang, S., Liu, S. and Feng, W., Journal of the mechanical behavior of biomedical materials. 4, 1228-1233 (2011).
55. Blum, M. M. and Ovaert, T. C., Journal of biomedical materials research. Part B, Applied biomaterials. 100, 1755-1763 (2012).
56. Katta, J. K., Marcolongo, M., Lowman, A. and Mansmann, K. A., Journal of biomedical materials research. Part A. 83, 471-479 (2007).
57. Shen, J. and Burgess, D. J., International journal of pharmaceutics. 422, 341-348 (2012).
58. D., S., DIABETES TECHNOLOGY & THERAPEUTICS. 6, 887-891 (2004).
59. Tibbitt, M. W. and Anseth, K. S., Biotechnology and bioengineering. 103, 655-663 (2009).
60. Sannino, A., Netti, P. A., Madaghiele, M., Coccoli, V., Luciani, A., Maffezzoli, A. and Nicolais, L., Journal of biomedical materials research. Part A. 79, 229-236 (2006).